Ultraintense X-Ray Induced Ionization, Dissociation, and Frustrated Absorption in Molecular Nitrogen

M. Hoener,[1,2] L. Fang,[1] O. Kornilov,[3] O. Gessner,[3] S. T. Pratt,[4] M. Gühr,[5] E. P. Kanter,[4] C. Blaga,[6] C. Bostedt,[7] J. D. Bozek,[7] P. H. Bucksbaum,[5] C. Buth,[5,8] M. Chen,[9] R. Coffee,[7] J. Cryan,[5] L. DiMauro,[6] M. Glownia,[5] E. Hosler,[10] E. Kukk,[11] S. R. Leone,[3,10] B. McFarland,[5] M. Messerschmidt,[7] B. Murphy,[1] V. Petrovic,[5] D. Rolles,[12] and N. Berrah[1,*]

[1]*Western Michigan University Physics Department, Kalamazoo, Michigan 49008, USA*
[2]*Advanced Light Source, Lawrence Berkeley National Laboratory, Berkeley, California 94720, USA*
[3]*Ultrafast X-ray Science Laboratory Chemical Sciences Division Lawrence Berkeley National Laboratory, Berkeley, California 94720, USA*
[4]*Argonne National Laboratory, Argonne, Illinois 60439, USA*
[5]*The PULSE Institute for Ultrafast Energy Science, SLAC National Accelerator Laboratory, Menlo Park, California 94025, USA*
[6]*The Ohio State University, Department of Physics, Columbus, Ohio 43210, USA*
[7]*Linac Coherent Light Source, SLAC National Accelerator Laboratory, Menlo Park, California 94025, USA*
[8]*Department of Physics, Louisiana State University, Baton Rouge, Louisiana 70803, USA*
[9]*Lawrence Livermore National Laboratory, Livermore, California 94550, USA*
[10]*Departments of Chemistry and Physics University of California, Berkeley, California 94710, USA*
[11]*Department of Physics and Astronomy, University of Turku 20014 Turku, Finland*
[12]*Max Planck Advanced Study Group, CFEL, 22761 Hamburg, Germany*

(Received 24 May 2010; published 23 June 2010)

Sequential multiple photoionization of the prototypical molecule N_2 is studied with femtosecond time resolution using the Linac Coherent Light Source (LCLS). A detailed picture of intense x-ray induced ionization and dissociation dynamics is revealed, including a molecular mechanism of frustrated absorption that suppresses the formation of high charge states at short pulse durations. The inverse scaling of the average target charge state with x-ray peak brightness has possible implications for single-pulse imaging applications.

DOI: 10.1103/PhysRevLett.104.253002 PACS numbers: 33.80.Rv, 32.80.Rm, 42.50.Hz

The development of femtosecond light sources covering the infrared to the extreme ultraviolet (EUV) has led to a revolution in time-resolved studies of physical and chemical processes [1]. However, even with the development of high-harmonic generation sources in the EUV and soft-x-ray regions, the relatively long wavelengths of these sources preclude the direct imaging of the motion of individual atoms. As a result, there has been a tremendous interest in ''fourth generation'' accelerator-based free electron lasers (FEL's) [2–6], which offer an unprecedented combination of spatial and temporal resolution. The Free Electron Laser in Hamburg (FLASH) [2–4] pushed the wavelengths of these sources into the soft x-ray regime, while the recently commissioned Linac Coherent Light Source (LCLS) now accesses the hard x-ray regime [4–6].

In this Letter, we present the first study of the response of a molecular system, N_2, to intense femtosecond duration laser pulses at a wavelength of 1.1 nm (1100 eV). We observe x-ray induced ionization and dissociation dynamics leading to various charge states up to fully-stripped N^{7+} ions. A molecular mechanism of frustrated absorption that suppresses the formation of high charge states at short pulse durations is revealed. We show that this phenomenon can be explained by a rate equation model that accounts for molecular valence electron dynamics during the sequence of ionization events. We also introduce a new parameter, the photon flux-weighted charge, $Q(\tau)$, which is a sensitive measure of the frustrated absorption.

The experiment was conducted using the LCLS Atomic Molecular and Optical (AMO) physics instrument [7]. The photon energy was $1100(\pm 15)$ eV with pulse durations of 280, 80, ~7, and ~4 fs [8,9]. Unless otherwise noted, the pulse energies quoted here are nominal values measured upstream from the beam line optics. These values are reduced by ~65%–85% in the interaction region due to photon beam transport losses [8]. The photon beam was focused by Kirkpatrick-Baez (KB) mirrors to an area equal to about 2 μm^2 [10]. Molecular N_2 was introduced into the instrument via a 100 μm pulsed nozzle. A time-of-flight (TOF) mass spectrometer [7] was used to analyze ions produced in the interaction of the sample with the LCLS pulses as shown in Fig. 1.

The x rays interact predominantly with the N_2 1*s* electrons, representing an entirely different regime than previous FEL-based experiments in the EUV [11]. Multiple cycles of photon absorption and Auger decay (PA processes) produce ions of increasing charge states, eventually reaching the extreme case where all electrons are removed. Absorption of five or more photons results in fully-stripped N^{7+} ions. These bare ions were indeed observed for long

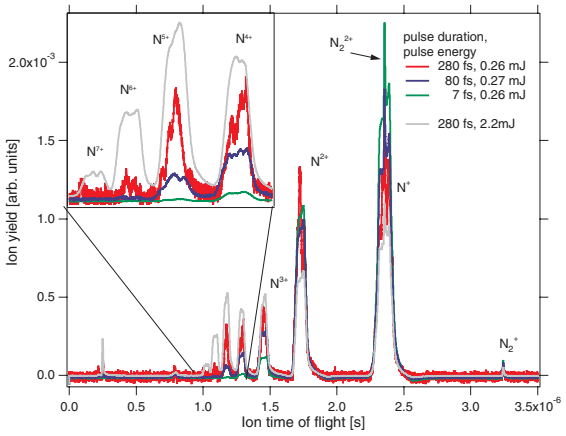

FIG. 1 (color online). Ion time-of-flight mass spectra of N_2 recorded at 1100 eV at three different pulse durations and similar pulse energies (~0.26 mJ, LCLS beam monitor). At long pulse durations and high pulse energies (280 fs, 2.2 mJ, gray curve) highly charged ions up to N^{7+} are observed.

(280 fs) pulses with high pulse energies (2.2 mJ), represented by the gray curve in Fig. 1. The high peak brightness of the LCLS also opens the novel possibility of creating double core holes (DCHs) by sequential two-photon absorption within the core-hole lifetime [9]. These DCH states of N_2 can have both holes on a single N atom, or a single hole on each atom.

The tremendous interest in single-pulse imaging and structure determination has raised questions about radiation damage and the ability to extract information before the sample is degenerated or destroyed [12]. Previous calculations and experiments have focused on the idea of ''inertial delay'' of the Coulomb explosion during scattering from a pulse that is significantly shorter than the disassembly time scale for the object [12–15]. In this letter we emphasize the importance of the detailed electronic dynamics in making a reliable estimate of image distortion effects, particularly for short pulses. The rate of ionization in the target induced by intense x rays governs the rate of electronic deterioration. Electronic damage, in turn, directly impacts both the scattering behavior of the sample and the extent of Coulomb repulsion that is ultimately responsible for the structural damage. Our work demonstrates that for sufficiently short pulses, frustrated absorption significantly reduces both the total photoionization cross section and the amount of Coulomb repulsion, and we can estimate this reduction quantitatively by using a parameterized rate equation model that takes into account interatomic valence electron dynamics.

Figure 1 shows ion time-of-flight spectra for three different pulse durations (~7 fs, 80 fs and 280 fs) at similar pulse energies (0.26 mJ). Over the range of parameters investigated, longer pulses result in the observation of the highest charge states (red curve) whereas shorter pulses lead almost exclusively to lower charge states. Highly charged N^{5+} and N^{6+} ions are clearly observed for 80 and 280 fs pulse lengths. In contrast, the ~7 fs spectrum shows only charge states up to N^{4+}. The intensity of the N^{3+}, N^{4+}, and N^{5+} peaks decreases monotonically from 280 fs pulse duration to ~7 fs pulse duration. This indicates that molecular N_2 and its fragments cannot absorb photons as efficiently for short pulses as for longer pulses.

The effect shown in Fig. 1 can be explained by frustrated absorption after the removal of K-shell electrons with a short pulse. The finite Auger relaxation time determines how fast the K shell can be replenished with electrons, and thereby limits the number of photons that can be absorbed in a given time interval. This leads to a reduction of multiple ionization events with increasing peak power and therefore a suppression of the production of higher charge states for short pulses.

To support this interpretation of the measurements, we have developed a theoretical description of the interaction of intense x rays with N_2 based on a parameterized rate equation model. Rate equation models have previously been applied to describe intense x-ray induced photoionization dynamics of independent atoms [13,16]. However, to our knowledge, no extension of this approach to molecular systems has been presented that includes interatomic valence charge dynamics.

Figures 2(a)–2(d) show the measured charge state distributions for four different x-ray pulse durations along with the results of the parameterized rate equation model. The average charge states $q_{\mathrm{av}}(\tau)$ shown in Fig. 2(e) are derived by $q_{\mathrm{av}}(\tau) = \sum_{i=1}^{7} N_i(\tau) q_i / \sum_{i=1}^{7} N_i(\tau)$ 1. Here, N_i are the relative abundances of the charge states q_i detected in the partial ion yield measurement. The relative ion yields have been corrected for the spectrometer-specific acceptance efficiency. Because of identical mass-to-charge ratios, the N^+ TOF peak contains a small (<2%) contribution from $N_2{}^{2+}$ ions, which is irrelevant for the results presented here. The frustrated absorption effect is clearly seen as a drop of the average charge with shorter pulse durations and it is well reproduced by the model calculations. Within the model, sequential multiple photoionization and relaxation of the molecule are described by a series of atomic photoionization and relaxation events. The final state of each ionization or relaxation event is modified such that the redistribution of valence charges amongst the two constituents of the molecule is included. All possible atomic core- and valence-shell ionization and relaxation channels are included, in particular, the production of double core holes (DCHs) in cases where a second core ionization takes place before an existing core hole has been refilled by Auger decay. The cross sections for the ionization processes and the lifetimes of the transient states are taken from [17]. Multielectron responses to a single photon, such as shake-up and shake-off processes, are not included. The temporal profile of the LCLS pulses is modeled by a random sequence of 1 fs duration subpulses with a rectangular pulse envelope that corresponds to the nominal pulse width. The spatial beam profile is approxi-

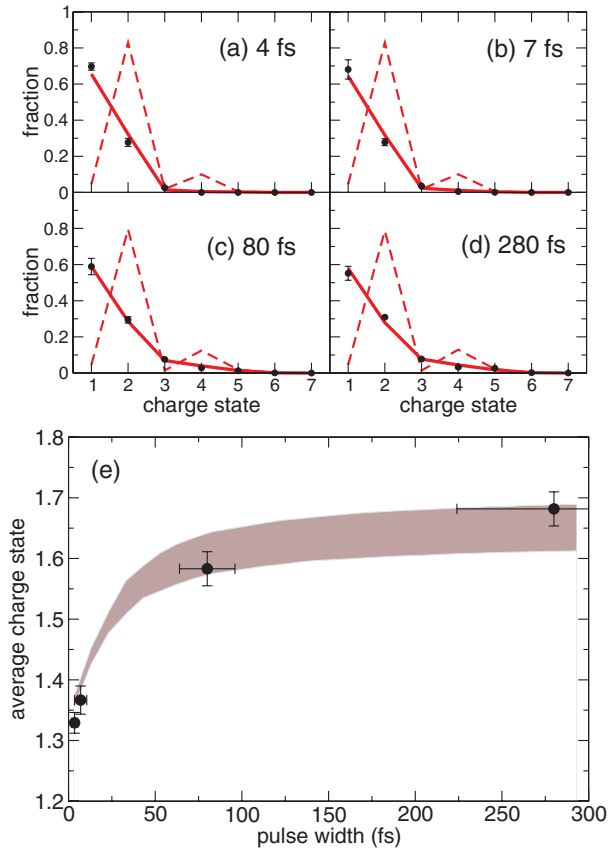

FIG. 2 (color online). (a)–(d) Charge state distributions and (e) average charge states of N^{n+} ions generated in the photoionization and relaxation of N_2 molecules using LCLS pulses with different pulse durations but constant pulse energy. The results of a rate equation model are shown as red lines (a)–(d) and a brown band (e), respectively. The results of an isolated atom-based rate equation model for a pulse energy of 49 μJ have been included as dashed lines in (a)–(d). See text for details.

mated by a Gaussian intensity distribution in accordance with the results of previous solid target depletion measurements [10].

The valence electron dynamics during exposure of N_2 to the pulse are included in the model by three parameters that govern the asymptotic valence charge distribution amongst the molecular constituents after fragmentation: (i) The ratio $(N^+\text{-}N^+)/(N\text{-}N^{2+})$ corresponding to the valence charge distribution after ionization and Auger decay of an initially neutral N_2 molecule (one PA cycle). (ii) The ratio $(N^{3+}\text{-}N^+)/(N^{2+}\text{-}N^{2+})$ corresponding to the distribution of 4 valence charges that result from a DCH decay. (iii) The ratio $(N^{3+}\text{-}N^+)/(N^{2+}\text{-}N^{2+})$ corresponding to the distribution of 4 valence charges that result from two sequential two PA cycles.

Ratio (i) is equivalent to the charge state distribution generated in the core ionization of N_2 at an x-ray source that induces no more than a single ionization event per molecule per pulse. Consequently, ratio (i) is set to the extrapolated value from the synchrotron-based photon-energy dependent N^+/N^{2+} fragment ion ratio of Ref. [18] at 1.1 keV. This ensures that the modeled charge state distributions converge to the correct values in the limit of low x-ray peak power densities.

The two $(N^{3+}\text{-}N^+)/(N^{2+}\text{-}N^{2+})$ ratios affect the relative charge sharing between the two atoms but not the average charge. The valence charge distribution induced by DCH decay is chosen to be completely symmetric, i.e., to result in a $N^{2+} + N^{2+}$. The choice of this ratio is based on the observation that for the shortest pulses ($\sim$4 fs), the contribution of N^{3+} ions to the total ion yield is almost negligible. In contrast, for the short pulse measurements, DCH relaxation is expected to contribute $\sim$7% or more to the total ion yield. If DCH relaxation results in significant N^{3+} ion production, the total N^{3+} yield would have to be significantly higher. This argument is independent of the type of core hole that is produced.

Ratio (iii) is adjusted to a value of 5 to generate the best overlap of the model with the results of the 280 fs pulse duration measurement. It is interesting that the derived ratio indicates an Auger relaxation in the second PA cycle that involves predominantly a single atom. This can be interpreted as resulting from fast progressing molecular dissociation initiated by the first Auger relaxation process that leads, on average, to atomic distances beyond the range where efficient charge transfer is taking place. This interpretation is supported by the fact that no other higher order (multiple photon) molecular contributions have to be included in the model to generate the good agreement with the data in Figs. 2(a)–2(d).

We emphasize that the theoretical curve presented in Fig. 2(e) is entirely defined by the experimental conditions and available spectroscopic data with no further adjustable parameters [only ratio (i) contributes]. As mentioned above, the beam line transmission is not well determined [10], leading to an uncertainty in the pulse energy at the sample. The model allows for a determination of the on-target pulse energy beyond the precision of the theoretical beam line transmission estimates. The brown band in Fig. 2(e) indicates the variation of the model calculations when adjusting the pulse energy between 17% and 21% of the nominal pulse energy (0.26 mJ). The good agreement of the band with the measured data indicates that the fundamental physics of the frustrated absorption effect is captured in the model. The width of the theory band is a measure of the precision with which the pulse energy at the sample can be determined within the rate equation model.

To demonstrate the importance of molecular valence charge dynamics in the modeling of charge formation, the results of a rate equation model that is entirely based on an independent atom picture are included in Figs. 2(a)–2(d) as dashed lines. This atomic model cannot reproduce even the qualitative features of the observed charge state distributions since, for example, the Auger decay of an atomic inner shell hole will always lead to a doubly or

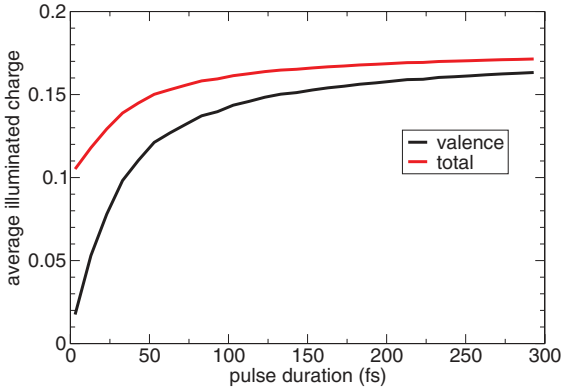

FIG. 3 (color online). Model calculation of the illuminated charge per atom as a function of pulse length (pulse energy: 49 μJ). For x-ray imaging experiments, this quantity should be as small as possible.

higher charged atom. The parameterized rate equation model describes the charge formation and frustrated absorption in N_2 exposed to intense x rays with encouraging accuracy. The inclusion of molecular valence electron dynamics in the theoretical description is instrumental to describe charge formation, and therefore damage formation, on the microscopic scale.

Beyond the fundamental importance of modeling a new regime of x-ray induced chemical dynamics, the ability to describe atom-specific transient charge formation in molecular samples will be vital to model damage mechanisms induced by the LCLS with Angström spatial resolution and femtosecond time resolution. Figure 3 provides a demonstration of how the findings described above can be employed to estimate charge-induced distortion effects in single-shot imaging of molecular samples. These distortion effects are directly related to the Coulomb repulsion between charged atoms within the molecular complex, and thus to the time-dependent charging of the sample. In contrast to the asymptotic charge distributions that define the partial ion yields described in Fig. 2, only those charges that are present at the moment that the photons pass through the sample are of interest for imaging applications. An important benchmark for the achievable image quality is therefore the photon flux-weighted charge as defined by $Q(\tau) = \int_{-\infty}^{+\infty} q(t) I_\tau(t) dt / \int_{-\infty}^{+\infty} I_\tau(t) dt$ 2. Here, $q(t)$ is the transient average charge in the molecule and $I_\tau(t)$ is the time-dependent intensity of the x-ray pulse with a pulse envelope width τ. It is important to distinguish between the quantities described in 1 and 2. The illuminated charge $Q(\tau)$ represents the average charge that is encountered by an imaging photon while it traverses the sample. $Q(\tau)$ is significantly more affected by frustrated absorption than the asymptotic average charge $q_{\mathrm{av}}(\tau)$ (Figs. 2 and 3). At a pulse energy of 49 μJ (19% of 0.26 mJ), corresponding to the experimental conditions described above, $Q(\tau)$ varies by ~40% if all charges are included in $q(t)$ and by ~90% if $q(t)$ is limited to the average valence charge. The illuminated valence charge is of particular interest since valence charges are predominantly responsible for distortion effects in the regime of low average charge. Core electrons contribute only little to molecular bonding. In addition, Coulomb repulsion between core holes that are shielded by a number of valence electrons is expected to be significantly smaller than the repulsion between valence charges. Thus, the results presented in Fig. 3 suggest that the relatively modest frustrated absorption effect presented in Fig. 2(e) might reduce the Coulomb forces that are ultimately responsible for target distortion during imaging applications by about 1 order of magnitude.

In summary, the results presented here highlight some of the new frontiers in molecular physics that can be explored with high-intensity x-ray FELs. We present a microscopic picture of charge formation on a femtosecond time-scale and frustrated absorption in molecules that includes the decisive x-ray induced valence electron dynamics. The inclusion of molecular valence charge dynamics is fundamental for a correct description of frustrated absorption and time-dependent distortion effects in molecules. The present results are a significant step towards understanding ultraintense x-ray induced physical processes and chemical dynamics in molecules. The predicted suppression of Coulomb repulsion effects in ultrashort x-ray pulses by 1 order of magnitude might have far reaching implications for single-shot imaging applications, which are amongst the most promising fields of research at 4th generation light sources.

This work was supported by the U.S. Department of Energy, Office of Science, Office of Basic Energy Sciences, Division of Chemical Sciences, Geosciences, and Biosciences. We thank R. Santra, R. Dörner, P. Emma, J. Frisch, and H. Zhiron for their assistance. Portions of this research were carried out at the Linac Coherent Light Source, a national user facility operated by Stanford University on behalf of the U.S. Department of Energy, Office of Basic Energy Sciences.

*Corresponding author.
nora.berrah@wmich.edu

[1] See, e.g., P. Hannaford, *Femtosecond Laser Spectroscopy*, Kluwer Ser. Prog. Lasers (Kluwer, Dordrecht, 2004); L. R. Khundkar and A. H. Zewail, Annu. Rev. Phys. Chem. **41**, 15 (1990); F. Krausz and M. Ivanov, Rev. Mod. Phys. **81**, 163 (2009).
[2] W. Ackermann *et al.*, Nat. Photon. **1**, 336 (2007).
[3] C. Gutt *et al.*, Phys. Rev. B **79**, 212406 (2009).
[4] N. Berrah *et al.*, J. Mod. Opt. (to be published).
[5] J. Feldhaus, J. Arthur, and J. Hastings, J. Phys. B **38**, S799 (2005).
[6] LCLS facilty, http://lcls.slac.stanford.edu/.
[7] J. Bozek, Eur. Phys. J. Special Topics **169**, 129 (2009).
[8] P. Emma *et al.* (to be published).
[9] L. Young *et al.* (to be published).
[10] J. Krzywinski *et al.* (to be published).

[11] Y. H. Jiang *et al.*, Phys. Rev. Lett. **102**, 123002 (2009).
[12] M. J. Bogan *et al.*, Nano Lett. **8**, 310 (2008).
[13] R. Neutze *et al.*, Nature (London) **406**, 752 (2000).
[14] S. Marchesini *et al.*, Nat. Photon. **2**, 560 (2008).
[15] H. N. Chapman *et al.*, Nature Phys. **2**, 839 (2006).
[16] N. Rohringer and R. Santra, Phys. Rev. A **76**, 033416 (2007).
[17] M. H. Chen *et al.*, Phys. Rev. A **19**, 2253 (1979).
[18] W. C. Stolte *et al.*, At. Data Nucl. Data Tables **69**, 171 (1998).